https://doi.org/10.5194/tc-2019-173
Preprint. Discussion started: 2 September 2019
© Author(s) 2019. CC BY 4.0 License.

The Cryosphere Discussions

GPS Interferometric Reflectometry measurements of ground surface elevation changes in permafrost areas in northern Canada

Jiahua Zhang[1], Lin Liu[1], Yufeng Hu[2]

[1]Earth System Science Programme, Faculty of Science, The Chinese University of Hong Kong, Hong Kong, 999077, China
[2]College of Geology Engineering and Geomatics, Chang'an University, Xian, 710000, China

Correspondence to: Jiahua Zhang (zhangjiahua@link.cuhk.edu.hk)

Abstract. Global Positioning System Interferometric Reflectometry (GPS-IR) is a relatively new technique which uses reflected GPS signals to measure surface elevation changes to study frozen ground dynamics. At present, more than 200 GPS stations are in continuous operation in the Northern Hemisphere permafrost areas. They were originally designed and maintained for tectonic and ionospheric studies. However, only one site in Barrow, Alaska has so far been used to study permafrost by GPS-IR. Moreover, GPS-IR has high requirements on ground surface condition, which needs to be open, flat, and homogeneous. In this study, we screen 3 major GPS networks in Canada and identify 12 out of 38 stations located in permafrost areas as useful ones where reliable reflectometry measurements can be obtained. We narrow our focus to 5 Canadian Active Control System stations and obtain their daily GPS-IR estimated surface elevation changes. We find that the ground surface subsided in Alert and Resolute Bay respectively by 0.79 ± 0.04 cm yr^{-1} (2012–2017) and 0.70 ± 0.02 cm yr^{-1} (2003–2014), but uplifted in Iqaluit by 0.35 ± 0.04 cm yr^{-1} (2010–2017). At the other two sites respectively in Repulse Bay and Baker Lake, the trends are not statistically significant. The linear trends of deformation were negatively correlated with those of the thaw indices in Alert, Resolute Bay, and Iqaluit. Furthermore, in Resolute Bay, we also find that the end-of-thaw elevations during 2003–2012 were highly negatively correlated with the square root of thaw indices. This study highlights multiple useful GPS stations in northern Canada, where multi-year, continuous, and daily GPS-IR estimated surface deformation can be obtained and used to study frozen ground dynamics at various temporal scales and across a broad region.

1 Introduction

Since the International Polar Year (2007–2009), permafrost has undergone a warming trend globally, with an average increase of ground temperature at or near the depth of zero annual amplitude by 0.29 ± 0.12 °C during 2007–2016 (Biskaborn et al., 2019; Romanovsky et al., 2010; Smith et al., 2010). Warming permafrost causes ground ice melting, active layer thickening, and the release of previously sequestered carbon (Brown et al., 2000; Trucco et al., 2012). It affects hydrological, geomorphological, and biogeochemical processes (Mackey, 1966; Shur and Jorgenson, 2007; Lantuit and Pollard, 2008; Kokelj and Jorgenson, 2013). Measuring and quantifying permafrost changes are crucial for understanding the

https://doi.org/10.5194/tc-2019-173
Preprint. Discussion started: 2 September 2019
© Author(s) 2019. CC BY 4.0 License.


dynamics of the active layer and near-surface permafrost (collectively called as frozen ground in this paper), studying the response of permafrost environments to climate change, and assessing the risk of permafrost changes to infrastructures.

Surface elevation changes can serve as an indicator of frozen ground changes. The freeze/thaw of frozen ground is associated with the phase transition of soil moisture, leading to ~9% change of ice volume, due to the density difference between water and ice. Such volume change in freeze/thaw cycle causes the ground surface to uplift or subside seasonally.

Surface deformation can be measured by either traditional benchmark-based methods or modern geodetic and remote sensing ones. The traditional methods use vertical tubes or pipes, anchored deep into the permafrost, as datum references of ground surface for repeat leveling surveys (Mackey, 1983). Modern methods include Interferometric Synthetic Aperture Radar (InSAR), Light Detection and Ranging (LiDAR), and Global Navigation Satellite System (GNSS) positioning. InSAR has been used to measure and quantify surface subsidence in various permafrost landforms (Liu et al., 2010, 2014, and 2015; Chen et al., 2018). However, InSAR suffers from coarse temporal resolutions and interferometric coherence loss. Furthermore, InSAR measurements need reference points where the surface deformation is known or assumed to be zero. LiDAR has been used to construct differential elevation models to investigate surface deformation (Jones et al., 2015). However, LiDAR surveys are usually conducted at annual or multi-annual intervals. GNSS positioning has also been used to measure and quantify surface subsidence and uplift (Little et al., 2003; Shiklomanov et al, 2013; Streletskiy et al., 2017). However, those GNSS surveys are usually conducted at the beginning or end of thaw seasons.

Global Positioning System Interferometric Reflectometry (GPS-IR) is a technique which uses reflected GPS signals to measure ground surface changes, such as elevation, soil moisture content, and vegetation growth condition (Larson, 2016, 2019). GPS-IR has been successfully used to study frozen ground dynamics by measuring surface deformation at one station in Barrow, Alaska (Liu and Larson, 2018; Hu et al., 2018). Compared with the aforementioned modern methods, GPS-IR measurements of surface elevation changes have higher temporal resolutions, usually at daily intervals. Their accuracies are on the order of a few centimeters (typically ~2 cm). Their spatial coverage is antenna-height dependent, e.g., 1000 m^2 for a 2-m-height antenna. Such spatial coverage fills a gap between regional-scale satellite observations and in situ point measurements. Furthermore, GPS-IR measurements are free of solid earth movement, such as glacier isostatic adjustment and plate movement (Liu and Larson, 2018). GPS-IR measurements are converted from the vertical distances between the antenna and the reflecting surface. As both the antenna and the surface are equally affected by solid earth movement, GPS-IR measurements can directly reflect frozen ground dynamics.

However, some limitations exist when using GPS-IR. This technique can only be used in certain surface conditions. It needs the reflecting surface to be open, nearly flat, and relatively homogeneous (Larson, 2016). In addition, when the ground is

https://doi.org/10.5194/tc-2019-173
Preprint. Discussion started: 2 September 2019
© Author(s) 2019. CC BY 4.0 License.


covered by snow, GPS-IR estimated surface elevation changes are mainly caused by snow depth variation. This implies that ground uplift in freezing season cannot be obtained by GPS-IR if the ground is covered by snow.

More than 200 GPS stations are continuously operating in permafrost areas in Northern Hemisphere (Fig. 1). Most of them are located in Alaska and Canada. Due to the public accessibility of GPS data, abundant weather records, and detailed geological surveys, we choose Canada as our study area. Due to the limitations of GPS-IR, we first design a three-step framework to identify useful stations under the same protocols and to ensure the reliability of measurements. We then screen all of the major public GPS networks in Canada to identify the usable stations, estimate surface deformation by GPS-IR, and use them in turn to study frozen ground dynamics.

In Sect. 2, we describe the mechanism of GPS-IR to measure surface elevation changes, the framework to identify useful GPS stations, and the datasets we used in this study. In Sect. 3, we present basic information of the identified useful GPS stations (e.g. monument condition and antenna height) and environment conditions of the study sites such as biome and surficial material. We then show the results of surface elevation changes in thaw seasons at the study sites in Sect. 4. In Sect. 5, we discuss the capability of GPS-IR results in revealing frozen ground dynamics in various temporal scales, their limitations in permafrost studies, and their potential for validating and calibrating space-borne InSAR measurements. We conclude by summarizing the results and findings.

2 Methodology

2.1 GPS Interferometric Reflectometry (GPS-IR)

Larson (2016 and 2019) presented the principle of GPS-IR and its applications in measuring snow depth, surface soil moisture, vegetation growth condition, and water level. However, the use of GPS-IR for studying permafrost was not explicitly presented. So, here, we describe how GPS-IR can be used to obtain surface elevation changes and their link to ground deformation in permafrost areas.

The input of GPS-IR is signal-to-noise ratio (SNR) data of GPS signals. SNR represents the strength of the received signal, and it is one of the observables recorded by GPS receivers. An SNR series, corresponding to a satellite rising/setting track at low satellite elevation angles (e.g., 5°–20° used in this study), oscillates with respect to the satellite elevation angle. The oscillating frequency mainly depends on the vertical distance between the antenna and the reflecting surface (called reflector height and denoted as H). If a GPS station is located above a smooth horizontal surface (e.g. Fig. 2), SNR can be expressed by a sinusoidal function of elevation angle e (Larson, 2016):

$$SNR = A(e)\sin\left(\frac{4\pi H}{\lambda}\sin e + \phi\right), \quad (1)$$

https://doi.org/10.5194/tc-2019-173
Preprint. Discussion started: 2 September 2019
© Author(s) 2019. CC BY 4.0 License.


where $A(e)$ is the oscillation amplitude, also varying with e; λ is the wavelength of the carrier wave of GPS signal; and ϕ is the phase. When taking $\sin e$ as an independent variable, the oscillating frequency is:

$$f = \frac{2H}{\lambda}, \quad (2)$$

If f is determined, H can be obtained numerically as

$$H = \frac{f\lambda}{2}, \quad (3)$$

In practice, we conduct Lomb-Scargle Periodogram analysis of an SNR series to obtain its frequency spectrum, use its peak value as the oscillating frequency f, and then obtain H. We use the software tools of GNSS Interferometric Reflectometry (Roesler and Larson, 2018).

As the monument is deep anchored (e.g. Fig. 2), the GPS antenna is stable with respect to the permafrost. The variation of the distance H only depends on the change in surface elevation. Surface uplift leads to decreasing H, and vice versa. The change of H is opposite to that of surface elevation (Liu and Larson, 2018). In practice, for the daily measurements of reflector height, we first assign minus signs to them and then remove the average to represent surface elevation changes.

2.2 A framework for identifying useful GPS stations for studying permafrost by GPS-IR

GPS-IR requires the ground surface to be open and relatively flat and smooth. To identify suitable ones from the existing GPS stations under the same protocols and to ensure the reliability of GPS-IR measurements, we have designed a three-step framework, which is described in detail as follows.

Step 1: Selecting GPS stations in permafrost areas

We first check whether permafrost is present where the GPS station is located. This step aims to identify the GPS stations in permafrost areas. We use the International Permafrost Association map compiled by Brown et al. (1997), which shows the spatial distribution of permafrost in the Northern Hemisphere.

Step 2: Estimating an azimuth range with an open, flat, and homogeneous ground surface

In this step, we aim to estimate an azimuth range, where the surface is open, nearly flat, and relatively homogeneous at each selected station in step 1. Normally, ground photos of a GPS station are taken as a part of metadata. In practice, we use ground photos and Google Earth images of a GPS site to check its surrounding environment, then estimate an azimuth range free of obstructions. We also use these images to recognize whether the selected surface is nearly planar and smooth. In Fig. S1, we present ground photos of two GPS stations as typical positive and negative examples respectively.

Step 3: Ensuring high reliability of GPS-IR measurements

https://doi.org/10.5194/tc-2019-173
Preprint. Discussion started: 2 September 2019
© Author(s) 2019. CC BY 4.0 License.


125 At present, 31 operational GPS satellites orbit around the Earth twice daily. Therefore, multiple SNR series are available within a day. In practice, for any given day, we first process all SNR series within the determined azimuth range and elevation angle range to obtain their H using the standard method summarized in Sect. 2.1. Then, we calculate their median and discard the ones deviating from the median by 0.25 m or more. Then we compute the mean value and the standard deviation (σ) of the remaining H, and remove those H deviating from the mean value by larger than 3σ as outliers. The final
130 retained H and their corresponding SNR series are regarded as reliable. We average the final retained H (denote the average as $\overline{H}$) to represent the vertical distance between the antenna and the reflecting surface on that day. The uncertainty of $\overline{H}$ is represented by its standard deviation. To further ensure the reliability of $\overline{H}$, a minimal number of 10 pieces of reliable SNR series are required.

2.3 Auxiliary dataset and information

135 To understand and interpret GPS-IR results, we use air temperature and snow depth at the study sites. These measurements are recorded by the nearest weather stations of GPS sites, and can be downloaded from Environment Canada (http://climate.weather.gc.ca/historical_data/search_historic_data_e.html). We also use borehole ground temperatures at the study sites, which are provided by the Global Terrestrial Network for Permafrost (http://gtnpdatabase.org/boreholes).

140 We also summarize the climate and environment information of the study sites, such as mean annual air/ground temperature (Ednie and Smith, 2015; Environment Canada, http://climate.weather.gc.ca/climate_normals/index_e.html), surficial material (Cruishank, 1971; Dredge, 1994; Taylor, 1982; Throop et al., 2010), and ground ice content of near-surface permafrost (O'Neill et al., 2019), to provide background information for reference.

3 Identified GPS stations and study sites

145 We have screened all of the three major GPS networks in Canada, namely Canadian Active Control System (CACS), Canadian High Arctic Ionospheric Network (CHAIN), and Portable Observatories for Lithospheric Analysis and Research Investigating Seismicity (POLARIS) (Fig. 3). CACS is a nationwide network and is maintained by the Geodetic Survey Division in conjunction with the Geological Survey of Canada (Lahaye et al., 2001). CHAIN was designed to investigate the impact of solar output on planetary environment (Jayachandran et al., 2009). The network is operated by the University of
150 New Brunswick. It consists of 25 GPS stations, of which three (KUGC, REPC, and QIKC) are shared with CACS. It is important to note that most of the receiver antennas of CHAIN stations are anchored onto the roofs of buildings. Consequently, the monuments may move due to the foundation instability and thermal expansion/contraction of buildings. When using these stations for GPS-IR studies, corrections for such instability should be conducted. POLARIS, operated by the University of Western Ontario, was initiated for mapping Earth structure and assessing earthquake hazards (Eaton et al.,
155 2005). It includes seven geodetic-quality GPS stations.

https://doi.org/10.5194/tc-2019-173
Preprint. Discussion started: 2 September 2019
© Author(s) 2019. CC BY 4.0 License.


Following the framework in Sect. 2.2, we identified 12 GPS stations out of 38 ones located in permafrost areas as suitable ones for GPS-IR studies. Table 1 gives their basic information, including locations, data time spans, and spatial coverages of GPS-IR measurements. Five of them are from CACS, and the rest are from CHAIN. None of the POLARIS stations was identified as suitable.

Given that the GPS-IR measurements of the CHAIN stations might be affected by the unstable buildings, in this study we present and interpret the measured elevation changes at the 5 identified CACS stations. They are all located in the Canadian Arctic. Figure 4 shows their ground photos.

In the Canadian Arctic, the climate is dominantly Polar climate due to high latitude. The biomes are mainly tundra and Arctic desert. Permafrost is continuous in this area, and normally its thickness increases with latitude. In the far north latitude of 75°, permafrost can be thicker than 500 m (Sladen, 2011). Ground temperatures at or near the depth of zero annual amplitude ranged from colder than -15 °C to warmer than -2 °C, and they decreased northward in concert with climate (Smith et al., 2013). During 2008–2014, ground temperatures at the depth of 15 m increased at an average rate of ~0.17 °C yr^{-1} at ten extensively distributed sites in the Canadian Arctic (Ednie and Smith, 2015). Thawing ice-rich permafrost has initiated wide-spread development of thermokarst landforms in this region, such as retrogressive thaw slump (Lantuit and Pollard, 2008; Kokelj et al., 2015) and active layer detachment (Lewkowicz and Harris, 2005; Lewkowicz and Way, 2019).

We summarize the basic regional information of the five sites respectively in Table 2, including biome, land cover, ground ice content of near-surface permafrost, mean annual air temperature (MAAT), and mean annual ground temperature (MAGT). In Alert and Resolute Bay, the biomes are both Arctic Desert due to the high latitude, and the land surfaces are dominantly bare soil. The biomes at the other three sites are all tundra. But, due to their specific locations, the ground surface is mainly bare soil in Repulse Bay, but is covered by a peat layer in Baker Lake, and is sparsely vegetated in Iqaluit.

4 Results: surface elevation changes measured by GPS-IR

We obtain multi-year and seasonal time series of surface elevation changes at the 5 CACS sites. In this study, we only present the measurements in the thaw seasons, when the air temperature is above 0 °C and the ground is not covered by snow. The measurements can be found in Zhang et al., 2019 (https://doi.pangaea.de/10.1594/PANGAEA.904347).

We build best linear fit lines to the thaw-season measurements and obtain the trends at the five sites (Fig. 5). We find that in Alert and Resolute Bay, the ground surface subsided at a rate of 0.79 ± 0.04 cm yr^{-1} (2012–2017) and 0.70 ± 0.02 cm yr^{-1} (2003–2014), respectively. By contrast, the ground surface uplifted in Iqaluit by 0.35 ± 0.04 cm yr^{-1} (2010–2017). However,

https://doi.org/10.5194/tc-2019-173
Preprint. Discussion started: 2 September 2019
© Author(s) 2019. CC BY 4.0 License.


at the other two sites, the displacements of the ground surface were 0.05 ± 0.08 cm yr^{-1} in Repulse Bay during 2014–2017, and 0.04 ± 0.02 cm yr^{-1} in Baker Lake during 2010–2017. These last two trends were not statistically significant (t-test, $p = 0.95$).

In Fig. 6, we present the seasonal surface elevation changes in Resolute Bay. The seasonal results of the other sites can be found in Fig. S2–S5. During a thaw season, the ground surface typically subsides progressively and reaches its lowest position at the end of season. However, at the Resolute Bay site, the surface elevation changes in the thaw seasons were irregular. The surface uplifted abnormally and significantly within the thaw seasons, for instance in 2003 and 2007. This phenomenon could be due to the refreezing of soil moisture which migrated from the thawed active layer, or the swelling of soil when it became wet. However, we lack measurements of soil moisture and ice content to investigate the cause of the observed uplift. Moreover, the elevation changes among the thaw seasons were inconsistent. Given the complexity of these seasonal elevation changes, we turn to investigate the interannual variability and linear trends of surface deformation in Resolute Bay.

5 Discussion

In this section, we first interpret GPS-IR measured surface elevation changes in Resolute Bay, as they are the longest among the five sites. We then qualitatively study the linear trends of surface deformation at the five sites. We also discuss the limitations of the use of GPS-IR measurements in permafrost studies, and their capability in validating and calibrating space-borne InSAR observations.

5.1 Interannual variability of end-of-thaw elevations in Resolute Bay

Net seasonal subsidence is an effective indicator of the response of frozen ground to the atmosphere, as it mainly depends on the soil moisture content within the active layer and the heat from the atmosphere. But, as shown in Sect. 4 and Fig. 6, it is challenging to reliably obtain seasonal subsidence in Resolute Bay due to the irregularity and inconsistency of surface elevation changes in thaw seasons. As an alternative, we use the end-of-thaw-season surface elevations to investigate the frozen ground dynamics.

The end-of-thaw elevation is determined as the mean value of the elevations at the last seven days of a thaw season, since the thawing front moves slowly at the end of thaw and the further surface deformation is limited. According to Stefan equation, the active layer thickness is approximately proportional to the square root of thaw index (Brown et al., 2000; Smith et al., 2009; French, 2017). Thaw index is represented by the degree days of thawing (DDT) derived by the accumulation of daily air temperatures above 0 °C till the end of thaw season. As surface subsidence is mainly caused by ice-melting within the active layer, we compare the end-of-thaw elevations to the square root of the annual thaw indices (Fig. 7).

https://doi.org/10.5194/tc-2019-173
Preprint. Discussion started: 2 September 2019
© Author(s) 2019. CC BY 4.0 License.


In Fig 7a, the end-of-thaw-season elevations and $\sqrt{DDT}$ were highly negatively correlated between 2003 and 2012, whereas the end-of-thaw elevations were low with cool summers in 2013 and 2014. To further investigate their correlation, we draw a scatter plot of end-of-thaw-season elevations versus $\sqrt{DDT}$ (Fig. 7b), but find that the linear line fitted poorly. After removing the measurements in 2013 and 2014, the R^2 and Root Mean Square Error (RMSE) of the best linear fit improves significantly, from 0.24 to 0.83 and 2.57 cm to 1.19 cm, respectively (Fig. 7c).

We postulate that the highly negative correlation between the end-of-thaw elevations and $\sqrt{DDT}$ during 2003–2012 was due to thickening active layer. A larger DDT indicates that more heat is available to penetrate into the deeper part of the frozen ground, leading to active layer thickening, more ice melting within the frozen ground, and thus larger subsidence and lower surface elevation. This assumption of thickening active layer during 2003–2012 is consistent with the borehole ground temperatures during 2008–2012 (Fig. 8). The ground temperatures showed that the thawing front (i.e., the 0 °C isotherm) deepened and exceeded 1 m depth in 2011.

However, in 2013 and 2014, the end-of-thaw elevations were low, even in the relatively cool summers (corresponding to low DDT). This is possibly due to the Markovian behavior of the active layer. Markovian behavior describes the reset of the active layer's response to air temperature after an extremely warm or cold summer, and this new response regime will last till the next extreme thaw season (Nelson et al., 1998). In Resolute Bay, the year 2011 had the warmest summer with the DDT of 542.9 °C•day, more than 4 times larger than that in 2004 (132.3 °C•day). After 2011, the response of active layer to the atmospheric forcing may have changed, due to the changes in thermal properties of the active layer and ice content at the permafrost table. So, even with low DDT, the maximal thaw depths were still larger than expected, resulting in low end-of-thaw-season surface elevations. Yet, ancillary data such as thermal properties, ice content, soil moisture, and thaw depth are needed to test these postulated changes in the active layer.

5.2 Linear trends of surface deformation at the CACS sites

The ground surface deformed differently among the five sites. In this subsection, we study the possible links between linear trends of surface deformation and air temperature, landcover, as well as ground ice near the permafrost table.

We make basic statistics of the annual thaw indices during the study periods at the sites of Alert, Resolute Bay, and Iqaluit (Table 3). Alert and Resolute Bay both had warming thaw seasons, with trends of 16.15 ± 0.20 °C•day yr^{-1} during 2012–2017 and 8.17 ± 0.07 °C•day yr^{-1} during 2003–2014, respectively. Conversely, the thaw season in Iqaluit underwent a cooling trend of 16.12 ± 0.18 °C•day yr^{-1} during 2010–2017.

https://doi.org/10.5194/tc-2019-173
Preprint. Discussion started: 2 September 2019
© Author(s) 2019. CC BY 4.0 License.


The ground surface underwent subsidence in Alert and Resolute Bay with increasing DDT, and uplift in Iqaluit with decreasing DDT. At these three sites, the surficial materials are sandy soil and barely vegetated (Table 2). Due to the lack of insulating organic layer, bare soil facilitates the heat transfer between the atmosphere and the ground. When the climate was warming, the transient layer (i.e. the layer between the active layer and long-term permafrost table and subjected to freeze and thaw seasonally to centennially (Shur et al., 2005)) started to thaw with ground ice melting and surface subsidence, such as that seen in Alert and Resolute Bay, even though they have low ice content in near-surface permafrost (Table 2). The opposite occurred in Iqaluit. The spatial difference of the trends of surface deformation also could be largely explained by the regional air temperature changes.

5.3 Limitations of GPS-IR measured surface deformation in permafrost studies

GPS-IR measured surface deformation has relatively large uncertainties, whose magnitudes are on the order of a few centimeters (i.e. ~2 cm in Resolute Bay). The uncertainties are mainly caused by the rugged surface, presence of vegetation, and other unexpected disturbances. Such uncertainties make it difficult to study the daily changes of surface elevation based on GPS-IR measurements, and even the seasonal changes if their magnitudes are comparable to those of seasonal subsidence. Resolute Bay is such a case, where daily and seasonal elevation changes cannot be obtained reliably. However, 12-years long measurements enable the interannual variability of end-of-thaw elevations and decadal linear trend to be obtained with high confidence.

Data gaps exist in GPS observations due to instrumental problems. GPS-IR measurements before and after the gaps are contaminated by the bias introduced by the replacement of instruments. The data gaps and bias hinder the study of permafrost with long-term, continuous, and consistent GPS-IR measurements.

The interpretation of GPS-IR measurements in permafrost areas needs ground observations, such as soil temperatures and moistures. However, these data are usually not available at GPS sites, as they were installed initially for tectonic and ionospheric research. Moreover, surface condition records are often brief or absent. This being the case, we usually only have GPS-IR measurements, and lack ancillary data such as ground temperature or soil moisture to help interpret the GPS-IR results.

These limitations indicate that, in the future, better location choices and maintenance of GPS stations and other ground measurement sensors are needed to exploit the full potential of GPS-IR observations in permafrost studies.

5.4 Potential of linking GPS-IR measurements to large-scale mapping from InSAR

Both GPS-IR and InSAR can measure surface elevation changes. In Table 4, we summarize their typical temporal and spatial samplings rates, advantages, and limitations. As we mentioned in Sect. 1, GPS-IR measurements are at daily intervals and

https://doi.org/10.5194/tc-2019-173
Preprint. Discussion started: 2 September 2019
© Author(s) 2019. CC BY 4.0 License.


local scales. In contrast, space-borne InSAR observations have much coarser temporal resolutions (the shortest to date being 6 days) and larger spatial scales (covering tens of kilometers), and also require a reference point with known surface deformation or assumed stable. These characteristics make GPS-IR and InSAR measurements complementary to each other. GPS-IR measurements could be used to overcome the limitations of InSAR observations. In particular, as GPS-IR measurements are continuously and at daily intervals over a few years to decades, they can provide baseline information for reference and can validate InSAR observations.

Several major research programs such as Arctic-Boreal Vulnerability Experiment (ABoVE), Next-Generation Ecosystem Experiments (NGEE), and European Space Agency Permafrost Climate Change Initiative (CCI) use remote sensing elevation changes (e.g., InSAR) to investigate permafrost dynamics. GPS-IR measurements can be used to calibrate and validate them and provide baseline information for historical, current, and future remote sensing measurement from air and space.

6 Conclusions

In this study, for the first time, we identify 12 useful GPS stations extensively distributed across the Canadian permafrost areas.

At the 5 identified CACS sites, we obtain their time series of elevation changes. The ground surface subsided in Alert by 0.79 ± 0.04 cm yr^{-1} during 2012–2017, and in Resolute Bay by 0.70 ± 0.02 cm yr^{-1} during 2003–2014. By contrast, it uplifted in Iqaluit by 0.35 ± 0.04 cm yr^{-1} during 2010–2017. At the other two sites of Repulse Bay and Baker Lake, the linear trends are not statistically significant. The trends at Alert, Resolute Bay, and Iqaluit are negatively correlated to those of annual thaw indices, i.e., warming thaw seasons in Alert and Resolute Bay led to surface subsidence, while the opposite occurred in Iqaluit. The spatial difference of these surface deformation trends could be largely explained by regional air temperature changes.

In Resolute Bay, we also find a highly negative correlation between the end-of-thaw elevations and the square-root of thaw indices during 2003–2012 and suspect that it was possibly due to active layer thickening under the warming thaw seasons. Continuous and daily measurements reveal the complexity of frozen ground dynamics, i.e. the irregularity and inconsistency of seasonal surface elevation changes in Resolute Bay. To further investigate the dynamics and mechanisms of frozen ground changes, it is important to measure other variables such as ground temperature, soil moisture, and ground ice content.

This study highlights 12 GPS stations useful for studying permafrost by GPS-IR, even though they were not originally designed or maintained for cryospheric studies. Our framework can be applied to GPS networks in other regions and nations

https://doi.org/10.5194/tc-2019-173
Preprint. Discussion started: 2 September 2019
© Author(s) 2019. CC BY 4.0 License.


to identify more usable GPS stations. Multi-year, continuous, and daily GPS-IR measurements of surface deformation obtained at those sites can be used to elucidate the dynamics of frozen ground and its response to climate variations at local and regional scales. They are also complementary to existing monitoring networks such as the Circumpolar Active Layer Monitoring network (CALM) and Global Terrestrial Network for Permafrost (GTN-P) programs. Moreover, the GPS-IR measurements can validate or calibrate remote sensing observations of elevation changes in permafrost area.

Code and data availability

The software tools of GNSS Interferometric Reflectometry is available from https://www.ngs.noaa.gov/gps-toolbox/GNSS-IR.htm. The SNR observations of CACS GPS sites are available from https://webapp.geod.nrcan.gc.ca/geod/data-donnees/cacs-scca.php?locale=en. The air temperature and snow depth measurements are available from http://climate.weather.gc.ca/historical_data/search_historic_data_e.html. The borehole ground temperature measurements are available from http://gtnpdatabase.org/boreholes. The GPS-IR measurements of surface elevation changes at Alert, Resolute Bay, Repulse Bay, Baker Lake, and Iqaluit in Canada are available from https://doi.pangaea.de/10.1594/PANGAEA.904347.

Author contribution

JZ identified the useful GPS stations for GPS-IR studies, conducted data processing to obtain results of surface elevation changes, performed results analysis, and wrote the manuscript. LL helped interpreting the results and revising the manuscript. YH guided using the software of GNSS Interferometric Reflectometry and assisted in data processing.

Competing interest

The authors declare that they have no conflict of interest.

Acknowledgments

We thank CACS, CHAIN, and POLARIS for providing GPS observation files, Environment Canada for weather records, and GTN-P for borehole ground temperatures. We thank Kristine Larson for guidance on GPS-IR and its applications, Sharon Smith for providing thoughtful comments on the interpretation of our results, Michael Craymer for providing ground photos of the GPS station RESO, and Richard Chadwick for the monument conditions of CHIAN stations. This study was supported by the Hong Kong Research Grants Council (CUHK14305618).

https://doi.org/10.5194/tc-2019-173
Preprint. Discussion started: 2 September 2019
© Author(s) 2019. CC BY 4.0 License.


References

340 Biskaborn, B. K., Smith, S. L. and Noetzli, J.: Permafrost is warming at a global scale, Nat. Commun., 10(1), 1–11, doi:10.1038/s41467-018-08240-4, 2019.

Brown, J., Ferrians Jr., O., Heginbottom, J., and Melnikov, E. (Eds.): Circum-Arctic map of permafrost and ground-ice conditions, Circum-Pacific Map Series CP-45, US Geological Survey, Reston, VA, USA, 1997.

Brown, J., Hinkel, K. M. and Nelson, F. E.: The circumpolar active layer monitoring (CALM) program: Research designs
345 and initial results, Polar Geogr., 24(3), 166–258, doi:10.1080/10889370009377698, 2000.

Chen, J., Liu, L., Zhang, T., Cao, B. and Lin, H.: Using Persistent Scatterer Interferometry to Map and Quantify Permafrost Thaw Subsidence: A Case Study of Eboling Mountain on the Qinghai-Tibet Plateau, J. Geophys. Res. Earth Surf., 123, 1–14, doi:10.1029/2018JF004618, 2018.

Cruickshank, J. G.: Soils and Terrain Units around Resolute, Cornwallis Island, Arctic, 24(3), 195–209, 1971.

350 Dredge, L. A.: Quaternary Geology of Southern Melville Peninsula, Nunavut: Surface Deposits, Glacial History, Environmental Geology, and Till Geology, Geological Survey of Canada., 2002.

Eaton, D. W., Adams, J., Asudeh, I., Atkinson, G. M., Bostock, M. G., Cassidy, J. F., Ferguson, I. J., Samson, C., Snyder, D. B., Tiampo, K. F. and Unsworth, M. J.: Investigating Canada's Lithosphere and earthquake hazards with portable arrays, Eos, Trans. Am. Geophys. Union, 86(17), 169–173, doi:10.1029/2005EO170001, 2005.

355 Ednie, M. and Smith, S. L.: Establishment of Community-based Permafrost Monitoring Sites, Baffin Region, Nunavut, in: Proceedings of the 63rd Canadian Geotechnical Conference & 6th Canadian Permafrost Conference, 1205–1211., 2010.

Hu, Y., Liu, L., Larson, K. M., Schaefer, K. M., Zhang, J. and Yao, Y.: GPS Interferometric Reflectometry Reveals Cyclic Elevation Changes in Thaw and Freezing Seasons in a Permafrost Area (Barrow, Alaska), Geophys. Res. Lett., 45(11), 5581–5589, doi:10.1029/2018GL077960, 2018.

360 French. H. M.: The Periglacial Environment, Wiley, New York, 2017.

Jayachandran, P. T., Langley, R. B., MacDougall, J. W., Mushini, S. C., Pokhotelov, D., Hamza, A. M., Mann, I. R., Milling, D. K., Kale, Z. C., Chadwick, R., Kelly, T., Danskin, D. W. and Carrano, C. S.: Canadian High Arctic Ionospheric Network (CHAIN), Radio Sci., 44(3), 1–10, doi:10.1029/2008RS004046, 2009.

Jones, B. M., Grosse, G., Arp, C. D., Miller, E., Liu, L., Hayes, D. J. and Larsen, C. F.: Recent Arctic tundra fire initiates
365 widespread thermokarst development, Sci. Rep., 5(15865), 1–13, doi:10.1038/srep15865, 2015.

Kokelj, S. V and Jorgenson, M. T.: Advances in Thermokarst Research, Permafr. Periglac. Process., 24(2), 108–119, doi:10.1002/ppp.1779, 2013.

Kokelj, S. V, Tunnicliffe, J., Lacelle, D., Lantz, T. C., Chin, K. S. and Fraser, R.: Increased precipitation drives mega slump development and destabilization of ice-rich permafrost terrain, northwestern Canada, Glob. Planet. Change, 129, 56–68,
370 doi.org/10.1016/j.gloplacha.2015.02.008, 2015.

© Author(s) 2019. CC BY 4.0 License.


Lahaye, F., Collins, P., Héroux, P., Daniels, M. and Popelar, J.: Using the Canadian Active Control System (CACS) for Real-Time Monitoring of GPS Receiver External Frequency Standards, in: Proceedings of the 14th International Technical Meeting of the Satellite Division of The Institute of Navigation (ION GPS 2001), Salt Lake City, UT., 2220–2228, 2001.

Lantuit, H. and Pollard, W. H.: Fifty years of coastal erosion and retrogressive thaw slump activity on Herschel Island, southern Beaufort Sea, Yukon Territory, Canada, Geomorphology, 95(1), 84–102, doi.org/10.1016/j.geomorph.2006.07.040, 2008.

Larson, K. M.: GPS interferometric reflectometry: applications to surface soil moisture, snow depth, and vegetation water content in the western United States, Wiley Interdiscip. Rev. Water, 3(6), 775–787, doi:10.1002/wat2.1167, 2016.

Larson, K. M.: Unanticipated Uses of the Global Positioning System, Annu. Rev. Earth Planet. Sci., 47(1), 19–40, doi:10.1146/annurev-earth-053018-060203, 2019.

Lewkowicz, A. and Harris, C.: Morphology and geotechnique of active-layer detachment failures in discontinuous and continuous permafrost, northern Canada., 2005.

Lewkowicz, A. G. and Way, R. G.: Extremes of summer climate trigger thousands of thermokarst landslides in a High Arctic environment, Nat. Commun., 10(1), 1329, doi:10.1038/s41467-019-09314-7, 2019.

Little, J. D., Sandall, H., Walegur, M. T. and Nelson, F. E.: Application of differential global positioning systems to monitor frost heave and thaw settlement in Tundra environments, Permafr. Periglac. Process., 14(4), 349–357, doi:10.1002/ppp.466, 2003.

Liu, L., Jafarov, E. E., Schaefer, K. M., Jones, B. M., Zebker, H. A., Williams, C. A., Rogan, J. and Zhang, T.: InSAR detects increase in surface subsidence caused by an Arctic tundra fire, Geophys. Res. Lett., 41(11), 3906–3913, doi:10.1002/2014GL060533, 2014.

Liu, L. and Larson, M.: Decadal changes of surface elevation over permafrost area estimated using reflected GPS signals, Cryosph., 12(2), 477–489, doi:10.5194/tc-12-477-2018, 2018.

Liu, L., Schaefer, K. M., Chen, A. C., Gusmeroli, A., Zebker, H. A. and Zhang, T.: Remote sensing measurements of thermokarst subsidence using InSAR, J. Geophys. Res. Earth Surf., 120(9), 1935–1948, doi:10.1002/2015JF003599, 2015.

Liu, L., Zhang, T. and Wahr, J.: InSAR measurements of surface deformation over permafrost on the North Slope of Alaska, J. Geophys. Res. Earth Surf., 115(F03023), doi:10.1029/2009JF001547, 2010.

Mackay, J. R.: Segregated epigenetic ice and slumps in permafrost, Mackenzie Delta area, NWT, Geogr. Bull., 8, 59–80.

Mackay, J. R.: Downward water movement into frozen ground, western arctic coast, Canada, Can. J. Earth Sci., 20(1), 120–134, doi:10.1139/e83-012, 1983.

Nelson, F. E., Outcalt, S. I., Brown, J., Shiklomanov, N. I. and Hinkel, K. M.: Spatial and Temporal Attributes of the Active-Layer Thickness Record, Barrow, Alaska, U.S.A., in: Proceedings of 7th International Conference on Permafrost, 797–802., 1998.

O'Neill, H. B., Wolfe, S. A. and Duchesne, C.: New ground ice maps for Canada using a paleogeographic modelling approach, Cryosphere, 13(3), 753–773, doi:10.5194/tc-13-753-2019, 2019.

© Author(s) 2019. CC BY 4.0 License.


405 Roesler, C. and Larson, K. M.: Software tools for GNSS interferometric reflectometry (GNSS-IR), GPS Solut., 22(3), 80, doi:10.1007/s10291-018-0744-8, 2018.

Romanovsky, V. E., Smith, S. L. and Christiansen, H. H.: Permafrost thermal state in the polar northern hemisphere during the international polar year 2007-2009: A synthesis, Permafr. Periglac. Process., 21(2), 106–116, doi:10.1002/ppp.689, 2010.

Shiklomanov, N. I., Streletskiy, D. A., Little, J. D. and Nelson, F. E.: Isotropic thaw subsidence in undisturbed permafrost
410 landscapes, Geophys. Res. Lett., 40(24), 6356–6361, doi:10.1002/2013GL058295, 2013.

Shur, Y., Hinkel, K. M. and Nelson, F. E.: The transient layer: Implications for geocryology and climate-change science, Permafr. Periglac. Process., 16(1), 5–17, doi:10.1002/ppp.518, 2005.

Shur, Y. L. and Jorgenson, M. T.: Patterns of permafrost formation and degradation in relation to climate and ecosystems, Permafr. Periglac. Process., 18(1), 7–19, doi:10.1002/ppp.582, 2007.

415 Sladen, W. E.: permafrost., 2011.Smith, S. L., Riseborough, D. W., Ednie, M. and Chartrand, J.: A map and summary database of permafrost temperatures in Nunavut, Canada., 2013.

Smith, S. L., Burgess, M. M. and Taylor, A. E.: High Arctic permafrost observatory at Alert, Nunavut–analysis of a 23 year data set, in: Proceedings of the 8th International Conference on Permafrost, 1073–1078., 2003.

Smith, S. L., Wolfe, S. A., Riseborough, D. W. and Nixon, F. M.: Active-Layer Characteristics and Summer Climatic
420 Indices, Mackenzie Valley, Northwest Territories, Canada, Permafr. Periglac. Process., 20, 201–220, doi:10.1002/ppp.651, 2009.

Smith, S. L., Romanovsky, V. E., Lewkowicz, A. G., Burn, C. R., Allard, M., Clow, G. D., Yoshikawa, K. and Throop, J.: Thermal state of permafrost in North America: A contribution to the international polar year, Permafr. Periglac. Process., 21(2), 117–135, doi:10.1002/ppp.690, 2010.

425 Smith, S. L., Riseborough, D. W., Ednie, M. and Chartrand, J.: A map and summary database of permafrost temperatures in Nunavut, Canada., 2013.

Streletskiy, D. A., Shiklomanov, N. I., Little, J. D., Nelson, F. E., Brown, J., Nyland, K. E. and Klene, A. E.: Thaw Subsidence in Undisturbed Tundra Landscapes, Barrow, Alaska, 1962–2015, Permafr. Periglac. Process., 28(3), 566–572, doi:10.1002/ppp.1918, 2017.

430 Taylor, A., Brown, R. J. E., Pilon, J. and Judge, A. S.: Permafrost and the shallow thermal regime at Alert, N.W.T, in Proceedings of the Fourth Canadian permafrost conference, pp. 12–22., 1982.

Throop, J., Smith, S. L. and Lewkowicz, A. G.: Observed recent changes in climate and permafrost temperatures at four sites in northern Canada, 63rd Can. Geotech. Conf. 6th Can. Permafr. Conf., (Figure 1), 1265–1272, 2010.

Trucco, C., Schuur, E. A. G., Natali, S. M., Belshe, E. F., Bracho, R. and Vogel, J.: Seven-year trends of CO2 exchange in a
435 tundra ecosystem affected by long-term permafrost thaw, J. Geophys. Res. Biogeosciences, 117(2), 1–12, doi:10.1029/2011JG001907, 2012.

Zhang, J., Liu, L. and Hu, Y.: Reflector heights measured by GPS-IR at Alert, Resolute Bay, Repulse Bay, Baker Lake, and Iqaluit in northern Canada, https://doi.pangaea.de/10.1594/PANGAEA.904347, 2019.

https://doi.org/10.5194/tc-2019-173
Preprint. Discussion started: 2 September 2019
© Author(s) 2019. CC BY 4.0 License.

Table 1. Basic information of the identified GPS stations

ID	Site name	GPS network	Latitude & Longitude (°)	Permafrost zonation	GPS antenna Monument	Data time span	Azimuth angle range used by GPS-IR	Antenna height (m)	Footprint radius (m)
ALRT	Alert	CACS	82.49, -62.34	Continuous	Metal pipes anchored deep into permafrost	2012–2017	270°–360°	1.9	61
RESO	Resolute Bay		74.69, -94.89	Continuous		2003–2014	0°–90°	2.3	67
REPL	Repulse Bay		66.52, -86.23	Continuous		2014–2017	150°–250°	2.0	61
BAKE	Baker Lake		64.32, -96.00	Continuous		2010–2017	0°–90°	1.2	49
IQAL	Iqaluit		63.76, -68.51	Continuous		2010–2017	30°–120°	1.7	57
PONC	Pond Inlet	CHAIN	72.69, -77.96	Continuous	Mounted on buildings	2008–2018	150°–240°	4.5	102
HALC	Hall Beach		68.77, -81.26	Continuous		2008–2018	180°–360°	3.7	90
IQAC	Iqaluit		63.74, -68.54	Continuous		2008–2018	200°–320°	4.0	94
RANC	Rankin Inlet		62.82, -92.11	Continuous		2014–2018	300°–150°	3.8	91
FSIC	Fort Simpson		61.76, -121.23	Discontinuous		2014–2018	150°–330°	3.9	93
FSMC	Fort Smith		60.03, -111.93	Sporadic		2014–2018	30°–120°	3.9	93
SANC	Sanikiluaq		56.54, -79.23	Discontinuous		2008–2018	135°–225°	3.4	85

https://doi.org/10.5194/tc-2019-173
Preprint. Discussion started: 2 September 2019
© Author(s) 2019. CC BY 4.0 License.

Table 2. Regional background of the study sites

	Canadian Forces Station Alert	Resolute Bay	Repulse Bay	Baker Lake	Iqaluit
Biome	Polar Desert	Polar Desert	Tundra	Tundra	Tundra
Landcover[a]	Mainly silts, sands, and shattered rocks filled with ice, ranging from 2.4 to 4 m thick (Taylor, 1982)	Rounded or sub-angular gravels and shelly and fine-grained sands (Cruishank, 1983)	Sands and silts ranging from 1 to 10 m thick (Dredge, 1994)	Coarse gravels and sands with low ice contents underneath a peat layer (Throop et al., 2010)	A thin till veneer with fairly well-developed soil, with sparse vegetation (Throop et al., 2010)
Ground ice content of near-surface permafrost[b]	None[e]	Negligible wedge ice and low segregated ice	None	Negligible wedge and segregated ice	Low wedge, segregated, and relict ice
MAAT[c] (°C)	-18.0	-15.7	-12.1	-11.8	-9.8
MAGT[d] (°C)	-11.1 – -14.4 (2007–2011)	-11.9 (2008–2012)	-8.2 (2009–2013)	-7.9 (2006–2007)	-5.6 – -7.1 (2003–2004 & 2011–2012)

a. The landcover information is for the areas around the boreholes, which are close to the identified GPS stations.
b. The ground ice contents are surficial material unit-based, which are simulated with surficial geology, deglaciation, paleo-vegetation, glacial lake and marine limits, and modern permafrost distribution (O'Neill et al., 2019).
c. MAAT refers to Mean Annual Air Temperature during 1981–2010 (Environment Canada, http://climate.weather.gc.ca/climate_normals/index_e.html).
d. MAGT refers to Mean Annual Ground Temperature at or near the depth of zero annual amplitude, except Repulse Bay (Smith et al., 2013). MAGT at Repulse Bay was at the depth of 15 m (Ednie and Smith, 2015).
e. Note that it is contrary to the field observations (Taylor, 1982) that found ground ice exists in the active layer and near-surface permafrost in Alert.

https://doi.org/10.5194/tc-2019-173
Preprint. Discussion started: 2 September 2019
© Author(s) 2019. CC BY 4.0 License.

Table 3. Basic statistics of annual DDT at Alert, Resolute Bay, and Iqaluit

Site	Data time span	Mean (°C•day)	Trend (°C•day yr^{-1})	Trend of surface deformation[a] (cm yr^{-1})
Alert	2012–2017	255.85	+16.15 ± 0.20	-0.79 ± 0.04
Resolute Bay	2003–2014	319.03	+8.17 ± 0.07	-0.70 ± 0.02
Iqaluit	2010–2017	736.51	-16.12 ± 0.18	+0.35 ± 0.04

a. Negative means subsidence, vice versa.

465

Table 4. Comparing GPS-IR and space-borne InSAR for measuring surface elevation changes in permafrost areas

	GPS-IR	Space-borne InSAR
Temporal sampling	daily	6 days to months
Spatial coverage	Local, site-specific (about 1000 m^2)	Large scale (typically tens to hundreds of kilometers)
Need reference of known deformation	No	Yes
Advantages	Daily and continuous; Free of reference; Free of solid earth movement	High accuracy (The magnitude of uncertainty is on the order of a few millimeters)
Limitations	Surface should be relatively flat and smooth.	Coarse temporal resolution; Loss of coherence; Requiring a reference point.

https://doi.org/10.5194/tc-2019-173
Preprint. Discussion started: 2 September 2019
© Author(s) 2019. CC BY 4.0 License.

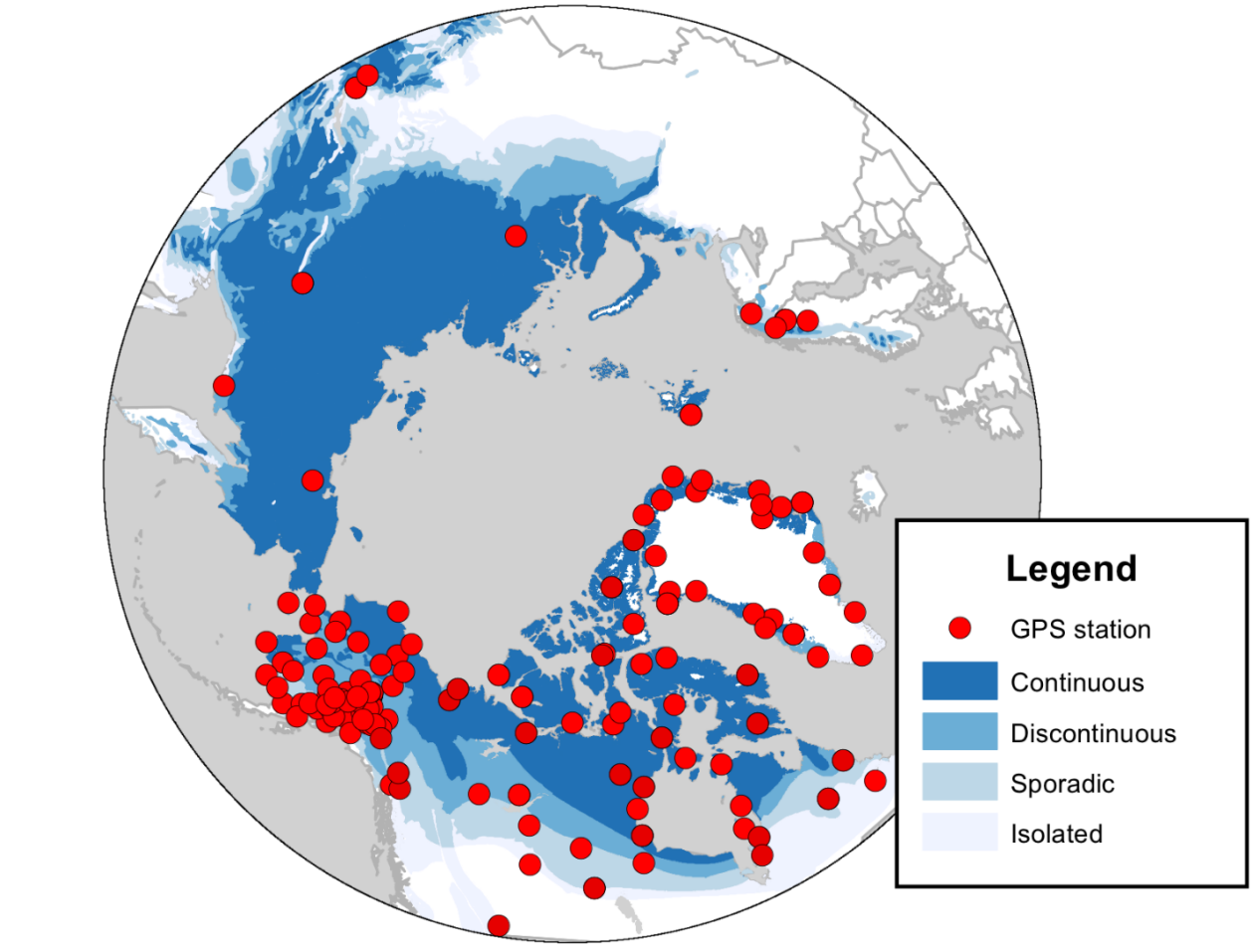

Figure 1: Locations of continuously operating and open-data GPS stations in the permafrost areas north of 50°N. The permafrost zonation, represented by various colors, is based on Brown et al. (1997).

https://doi.org/10.5194/tc-2019-173
Preprint. Discussion started: 2 September 2019
© Author(s) 2019. CC BY 4.0 License.

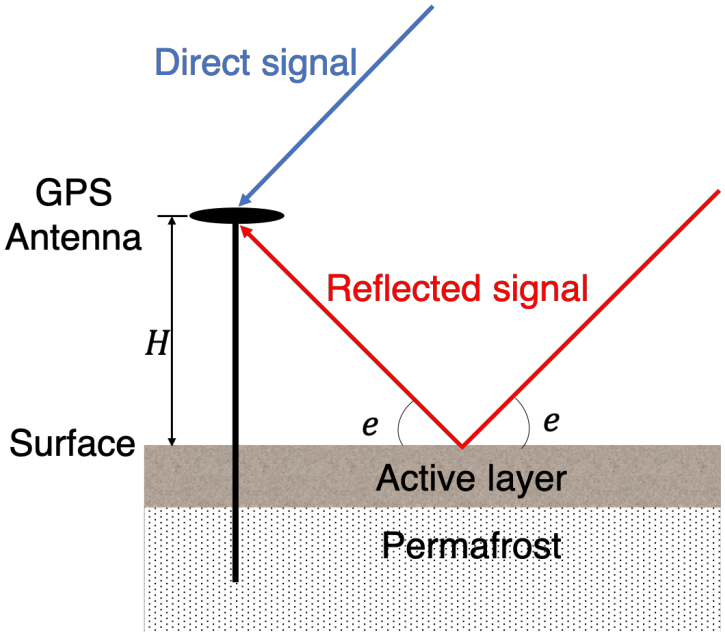

Figure 2: Schematic diagram showing the geometry of the GPS antenna, GPS signals, and the ground surface in permafrost area. *H*, or reflector height, is the vertical distance between the GPS antenna and the surface, and *e* is the satellite elevation angle.

https://doi.org/10.5194/tc-2019-173
Preprint. Discussion started: 2 September 2019
© Author(s) 2019. CC BY 4.0 License.

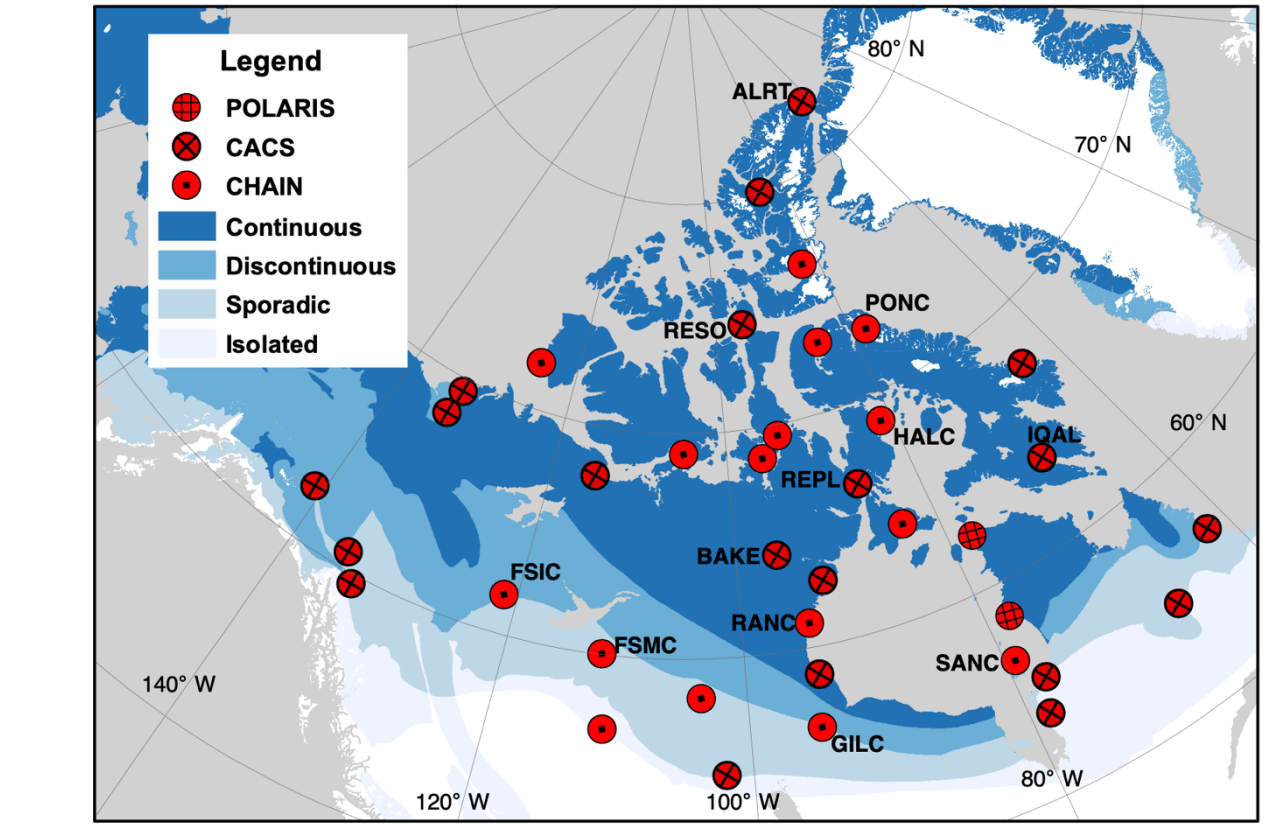

475

Figure 3: Locations of GPS stations in the Canadian permafrost areas. The identified stations are labeled by their four-character IDs.

https://doi.org/10.5194/tc-2019-173
Preprint. Discussion started: 2 September 2019
© Author(s) 2019. CC BY 4.0 License.

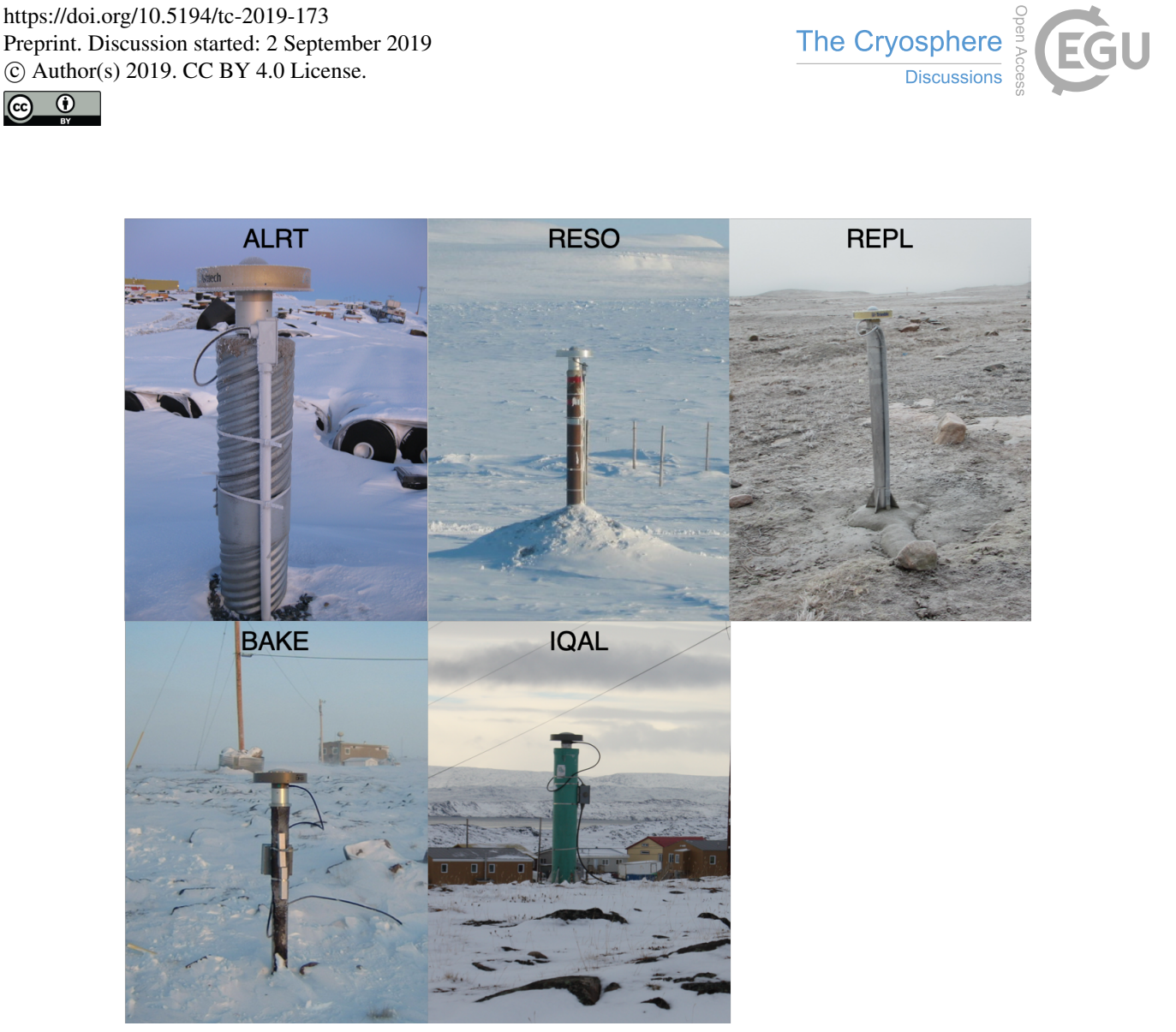

480 **Figure 4: Ground photos of the identified CACS GPS stations. Source: https://webapp.geod.nrcan.gc.ca/geod/data-donnees/cacs-scca.php?locale=en**

https://doi.org/10.5194/tc-2019-173
Preprint. Discussion started: 2 September 2019
© Author(s) 2019. CC BY 4.0 License.

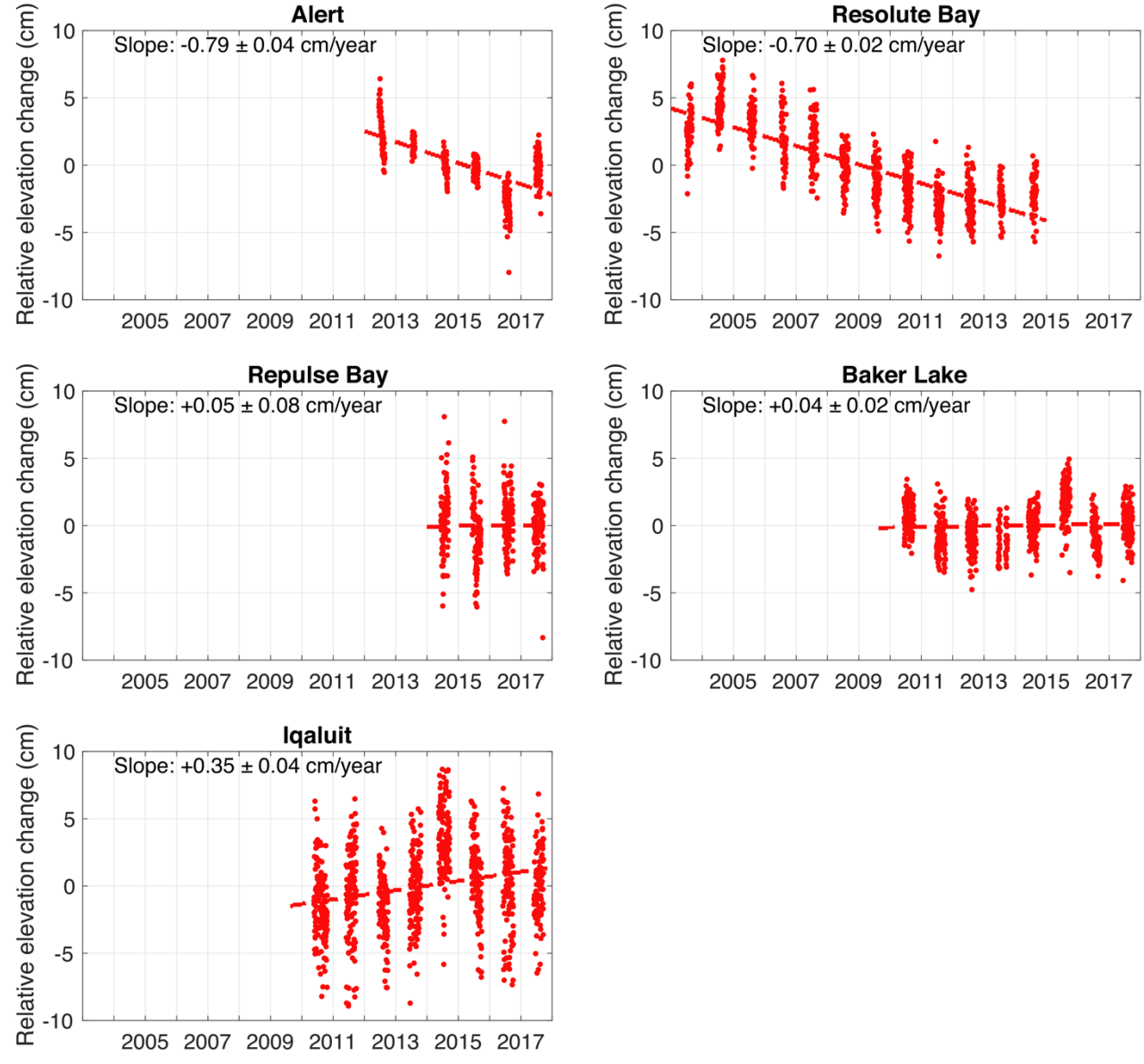

Figure 5: Time series and the best linear fit dashed lines of surface elevation changes in thaw seasons at the five CACS sites. For clarity, we do not show the error bars. For the y-axis, 'relative' means that the presented elevation changes are referenced to the mean value of the entire records at each site.

https://doi.org/10.5194/tc-2019-173
Preprint. Discussion started: 2 September 2019
© Author(s) 2019. CC BY 4.0 License.

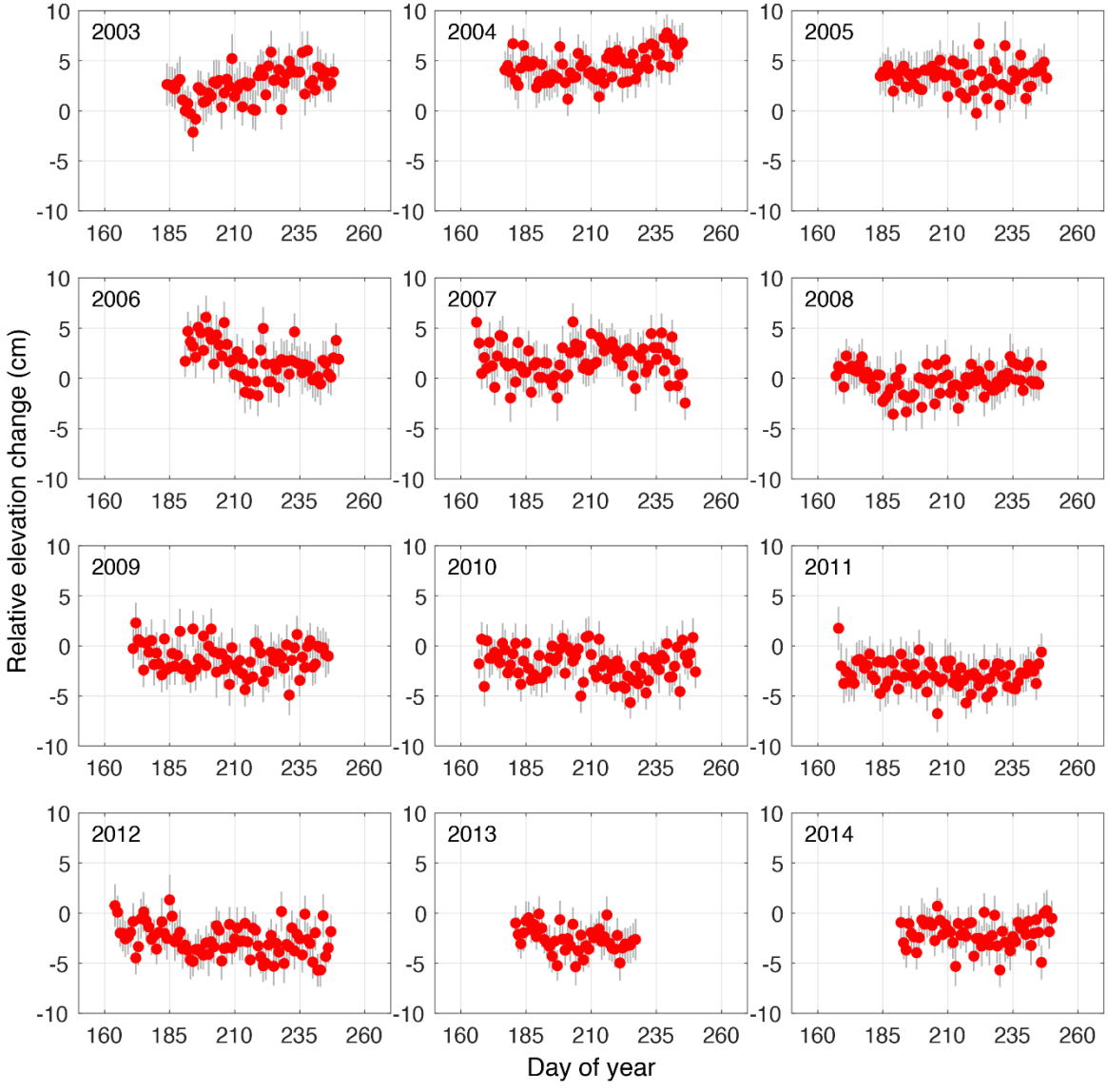

Figure 6: Surface elevation changes in each thaw season in Resolute Bay during 2003–2014. Red dots denote the measurements in the thaw seasons. Grey error bars denote the uncertainties. The mean value of the measurements has been removed. The shorter thaw season in 2013 was due to the late thawing onset on DOY 181 and early freezing onset on DOY 227, estimated from air temperature and snow depth records.

https://doi.org/10.5194/tc-2019-173
Preprint. Discussion started: 2 September 2019
© Author(s) 2019. CC BY 4.0 License.

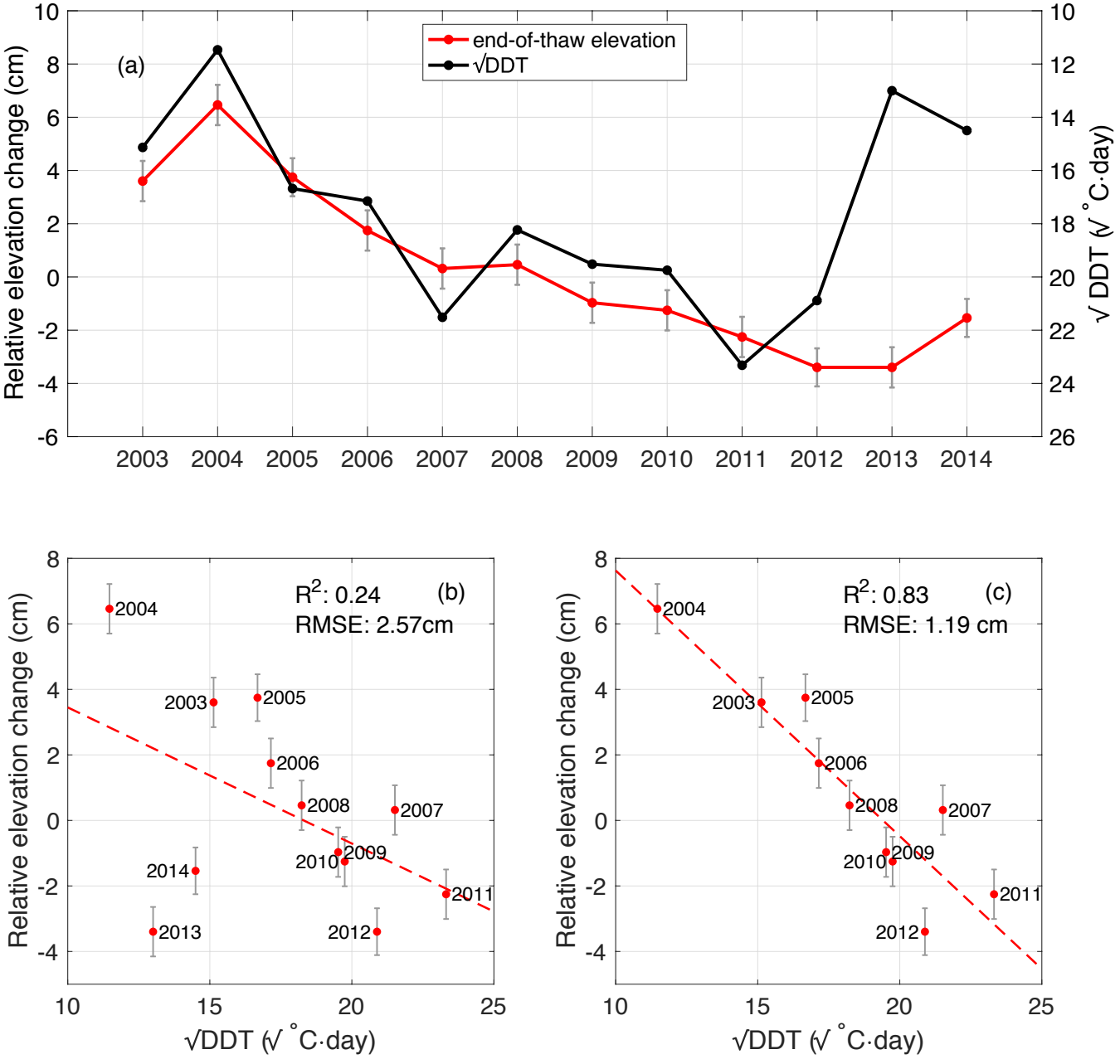

Figure 7: (a) Time series of the end-of-thaw-season elevations and $\sqrt{DDT}$ during 2003–2014. The right vertical axis for $\sqrt{DDT}$ has been reversed to show the correlation between $\sqrt{DDT}$ and the end-of-thaw elevations. (b) Scatter plots of the end-of-thaw elevations versus $\sqrt{DDT}$. The red dashed line is the best linear fit line. (c) Scatter plot and the best linear fit line of the end-of-thaw-season elevations vs $\sqrt{DDT}$ after removing the measurements of 2013 and 2014.

https://doi.org/10.5194/tc-2019-173
Preprint. Discussion started: 2 September 2019
© Author(s) 2019. CC BY 4.0 License.

The Cryosphere
Discussions
Open Access
EGU

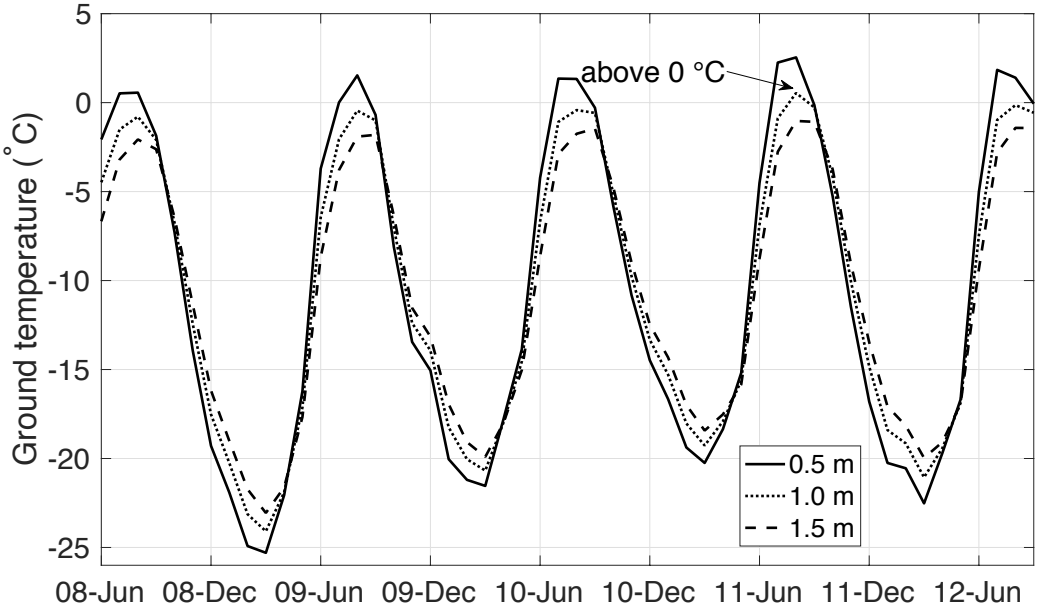

Figure 8: Time series of monthly ground temperatures at depths of 0.5 m, 1.0 m, and 1.5 m from June 2008 to September 2012 (Ednie and Smith, 2015). In August 2011, the ground temperature at 1.0 m depth was above 0 °C.